Synthesis and Characterization of Nanocrystalline $Ni_{1-x}Zn_xFe_2O_4$ ($0 \leq x \leq 0.5$) Spinel Ferrite Magnetic Material by Sol-Gel Auto-Combustion Method

K. Anitha Rani[1] and V. Senthil Kumar[1]

[1]Department of Physics, Karpagam University, Coimbatore-641021.

***Corresponding Author: Anitha Rani. K[1]**

ABSTRACT

Nanocrystalline powders of Ni-Zn ferrites, having chemical formula $Ni_{1-x}Zn_xFe_2O_4$ ($0 \leq x \leq 0.5$) were synthesized by using sol-gel auto-combustion method and annealed at 800°C for 5hrs. Studies using X-ray Diffraction (XRD), Fourier Transform Infra-Red Spectroscopy (FTIR), Scanning Electron Microscopy (SEM), Vibrating Sample Magnetometer (VSM) were carried out in order to characterize the structural, morphological, and magnetic properties of the resulting samples. The XRD spectra confirmed the formation of single-phase spinel cubic structure for all the prepared samples. The results of the FTIR analysis indicated that the functional groups of Ni-Zn spinel ferrite have intrinsic cation vibrations of the spinel structure. Furthermore, SEM micrograph showed uniformly distributed homogeneous nanoparticles grown by auto-combustion process. Moreover, it was found from VSM analysis that the values of the saturation magnetization increases by increasing the Zn content.

Key words: Ni-Zn ferrite, XRD, magnetic properties, sol-gel auto-combustion synthesis.

INTRODUCTION

During the past few decades spinel ferrites have become interesting research area, because of their wide range of applications in various fields such as electrical components, memory devices, microwave devices, transformers, inductors, choke, noise filters, magnetic recording heads, TV sets and portable radios etc [1]. Different chemical processing techniques are available for the preparation of ferrite powders, such as microwave refluxing [2], sol-gel [3-6], hydrothermal [7-8], co-precipitation [9] and spray pyrolysis [10]. Among these methods sol-gel auto-combustion method has numerous advantages over other chemical methods for the preparation of nanocrystalline ferrite powders [11].

Numerous studies on the effect of additive Ni-Zn ferrites have been reported in literature. The impact of terbium contents on magnetic, ferromagnetic resonance, electrical

and dielectric properties of $Ni_{1-x}Tb_xFe_2O_4$ ferrites has been investigated by Muhammad Azhar Khan *et al.*, [12]. From the results it was inferred that the coercive force and saturation magnetization decrease when terbium content is increased, which may be attributed to spin canting. Ali Ghasemi *et al*., [13] have synthesized $Ni_{0.6}Zn_{0.6}Fe_{2-x}Cr_{x/2}Al_{x/2}O_4$ powder by using conventional sol-gel method and evaluated its structural and magnetic properties. They found that the magnetization decreases when the substitution increases, due to occupation of Al and Cr cations at low level substitution in octahedral sites. A.T. Raghaender *et al*., [14] synthesized Al-doped nickel ferrite ($NiFe_{2-x}Al_xO_4$) powder by using sol-gel auto-ignition method and studied the effect of non-magnetic Al content on the structural and magnetic properties. It is confirmed that the hysteresis is decreased when the particle size was decreased. Khalid Mujasam Batoo *et al*., [15] prepared $Ni_{0.7-x}Mg_xCu_{0.3}Fe_2O_4$ ferrites powders by sol-gel method and studied the electrical and magnetic properties. From the TEM results it is found that the average particle size of the proposed material is between 40-50 nm. It is also clear from the magnetization studies that the magnetic moment of Ni-Cu-Mg nanoparticles decreases with increasing Mg^{2+} doping content. Few other researchers prepared $Ni_{0.5}Li_{1-2x}Cu_xFe_2O_4$ [16] and $Ni_xFe_{2-x}Bi_xO_4$ [17] nanopowders by using the sol-gel auto-combustion method. The sol-gel auto-combustion method is a very simple methodology to prepare the nanosized ferrites with better homogeneity at low, as well as high temperatures.

In the present investigation, we have employed sol-gel auto-combustion method to synthesize Ni-Zn ferrite nanocrystalline particles with different ratio (0.1, 0.3 and 0.5) and analyzed the characterization of nanocrystalline $Ni_{1-x}Zn_xFe_2O_4$ ($0 \leq x \leq 0.5$) spinel ferrite magnetic material.

MATERIAL AND METHODS

Experimental Procedure

Precursor samples of $Ni_{1-x}Zn_xFe_2O_4$ ($0 \leq x \leq 0.5$) nanoparticles were prepared by sol-gel auto-combustion method at 90^{o}C. All the chemicals purchased were of analytical grade, and were used as such without further purification. An aqueous solution of metal nitrates of nickel nitrate Ni $(NO_3)_2.6H_2O$, zinc nitrate Zn $(NO_3)_2.6H_2O$ and iron nitrate Fe $(NO_3)_3.9H_2O$ were dissolved separately in de-ionized water. The entire nitrate solutions were mixed together using a magnetic stirrer for 1 hour, at 50^{o}C. Citric acid ($C_6H_8O_7.H_2O$) was added to the prepared aqueous solution as a fuel, and as a better complexing agent. Also it helps to have controlled combustion reaction at low temperature. The molar ratio of metal nitrates to citric acid was 1:3. The mixed solution was neutralized by adding ammonia. As synthesized temperature reached 90^{o}C, a viscous gel formation occurred. The solution was kept at 90^{o}C for complete removal of solvent to get desired ferrite powder. Flower like voluminous and fluffy powder of ferrite powder was formed during auto-combustion process. After cooling, this was made into fine powder by grinding. The prepared ferrite fine powder was kept at 800^{o}C for 5 hrs for further investigations.

RESULTS AND DISCUSSION

Structural properties

1. X-ray Diffraction

Fig.1 shows the XRD patterns of the synthesized samples of $Ni_{1-x}Zn_xFe_2O_4$ ($0 \leq x \leq 0.5$) annealed at 800°C which confirms the single phase cubic structure without identification of secondary phase. All the reflection peaks were identified from the standard JCPDS card number – 74-2081. The crystallite size (D) for each sample was calculated by using the Debye-Sherrer formula,

$$D = 0.9\lambda/\beta cos\theta \quad (1)$$

where λ is the X-Ray wavelength (1.54060 Å), β is the full width at half maximum (FWHM) and θ is the Bragg's angle. The lattice constants (a) were determined by using this formula,

$$a = d_{hkl}(h^2 + k^2 + l^2)^{1/2} \quad (2)$$

The crystallite size of samples were calculated from (311) plane and was found that increases in zinc content there observed a decrease in its size from 59 to 27 nm. Moreover, the lattice constant also increased from 0.8323 to 0.8399 nm. This lattice expansion was only due to the larger ionic radii of Zn^{2+} (0.82 Å) as compared to Ni^{2+} (0.67 Å). Hence our results of all parameters are in good agreement with M. Atif et al [18].

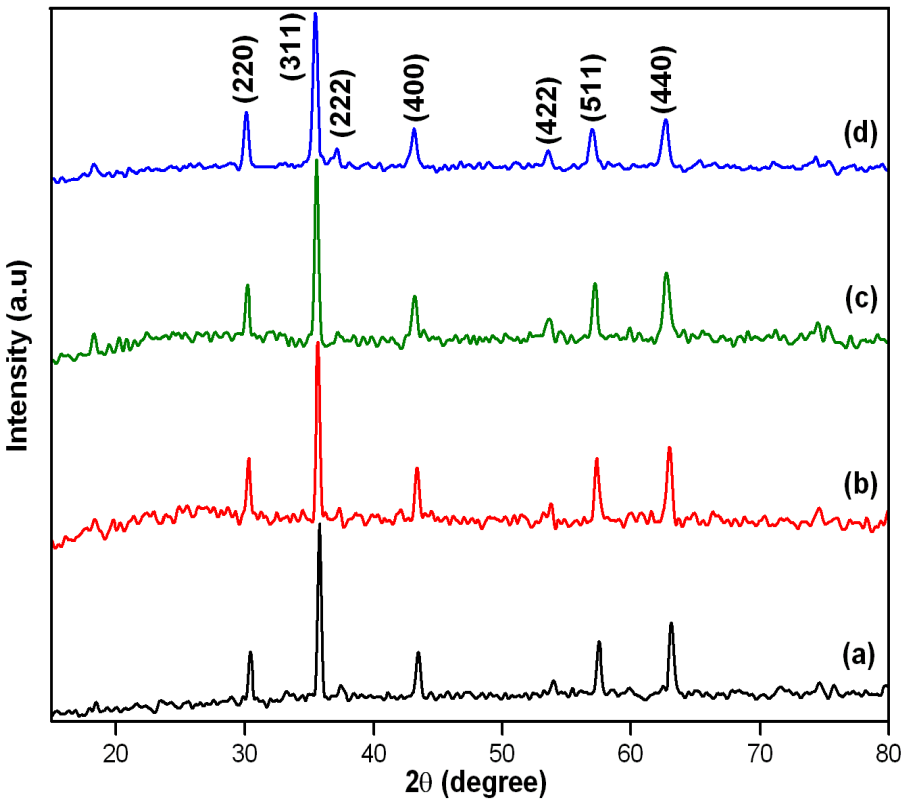

Fig. 1 X-ray diffraction patterns for (a) $NiFe_2O_4$ (b) $Ni_{0.9}Zn_{0.1}Fe_2O_4$ (c) $Ni_{0.7}Zn_{0.3}Fe_2O_4$ (d) $Ni_{0.5}Zn_{0.5}Fe_2O_4$ powders annealed at 800°C

2. Fourier Transform Infrared spectroscopy

Fig. 2 shows the FTIR absorption bands for $Ni_{1-x}Zn_xFe_2O_4$ ($0 \leq x \leq 0.5$) spinel ferrites at room temperature, in the range from 400 – 2600 cm^{-1}. It is obvious that, only four absorption bands are present. The two strongest absorption peaks lies in the range 410 – 585 cm^{-1} are due to the intrinsic stretching vibrations between tetrahedral metal ions and oxygen ions, and the remaining two weak peaks lies in the range 1560 – 2280 cm^{-1} are due to the stretching vibrations between octahedral metal ions and oxygen ions. Hence the two strongest peaks confirmed the spinel structure of all samples. Due to difference in Fe^{3+} - O^{2-} distances for the tetrahedral and octahedral sites, change in zinc content when the values of x increases, the position and intensities were changed.

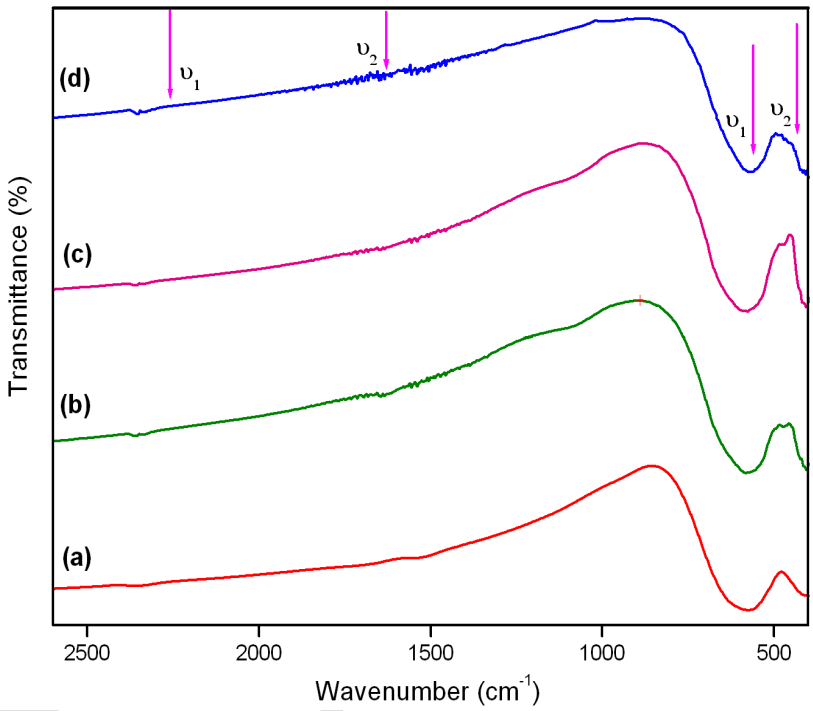

Fig.2 FTIR spectra of (a) $NiFe_2O_4$ (b) $Ni_{0.9}Zn_{0.1}Fe_2O_4$ (c) $Ni_{0.7}Zn_{0.3}Fe_2O_4$ (d) $Ni_{0.5}Zn_{0.5}Fe_2O_4$ powders annealed at 800°C

Morphological Properties

3. Scanning Electron Microscope

The morphology of the prepared nanomaterials ($Ni_{1-x}Zn_xFe_2O_4$) was determined by Scanning Electron Microscopy (SEM). The SEM images of $Ni_{1-x}Zn_xFe_2O_4$ ($0 \leq x \leq 0.5$) annealed at 800°C are shown in Fig.3. It is observed that, there is a uniform growth of nanocrystalline grains with Zn substitution, and increase in porosity. But for a change of the value of x from 0.1 to 0.3 in the sample, formation of a well defined, uniformly distributed, porous and few sphere like structures were observed. $Ni_{0.5}Zn_{0.5}Fe_2O_4$ shows the formation of honey comb like structure with large number of pores, due to gas release of combustion process [19].

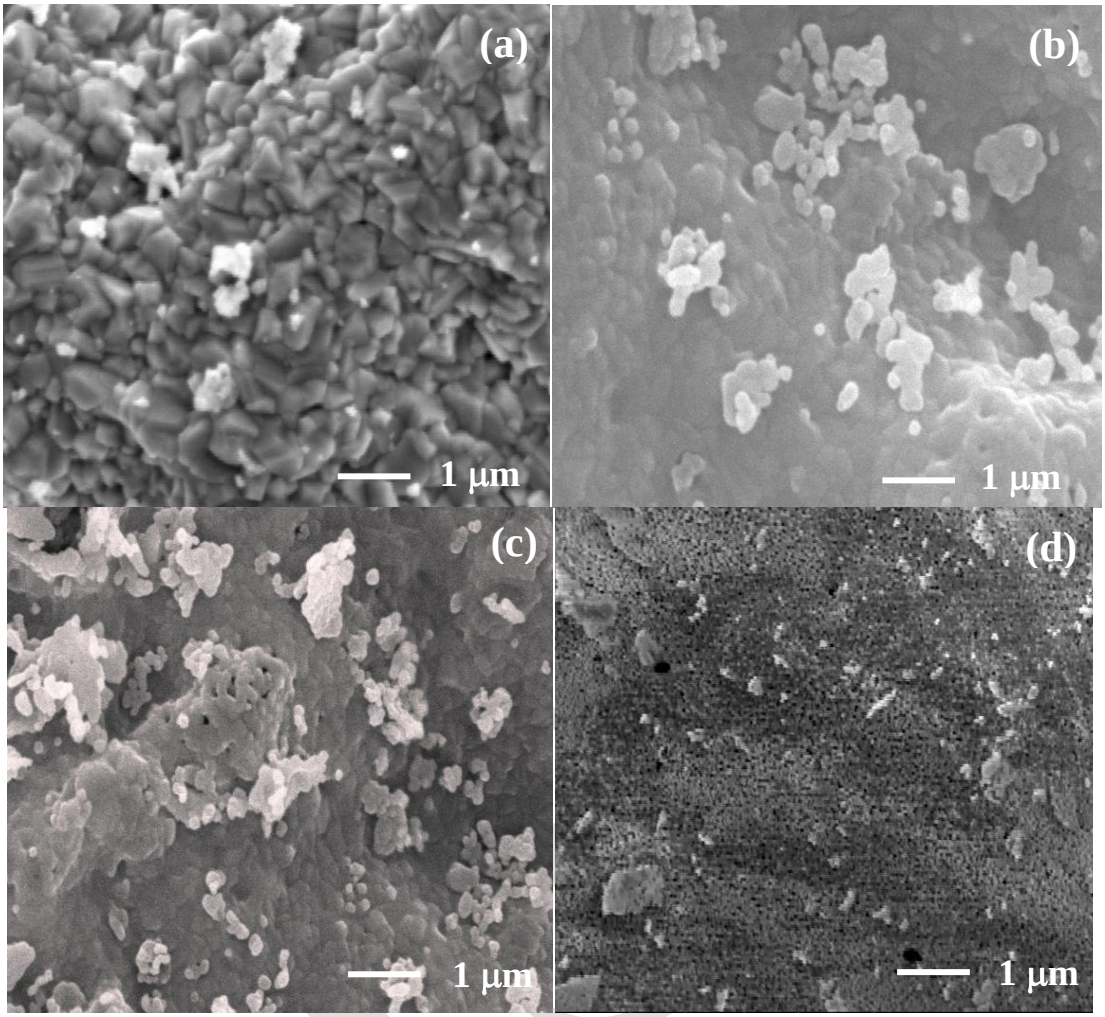

Fig.3 SEM micrographs of (a) $NiFe_2O_4$ (b) $Ni_{0.9}Zn_{0.1}Fe_2O_4$ (c) $Ni_{0.7}Zn_{0.3}Fe_2O_4$ (d) $Ni_{0.5}Zn_{0.5}Fe_2O_4$ powders annealed at 800^{o}C

Magnetic Properties

4. Vibrating Sample Magnetometer

The magnetic properties of all samples were studied by using VSM at room temperature, and magnetization of $Ni_{1-x}Zn_xFe_2O_4$ ($0 \leq x \leq 0.5$) samples annealed at 800^{o}C was observed at an applied field of 18 kOe. The saturation magnetization (M_s), coercivity (H_c), and remanent magnetization (M_r) of these materials were determined from the hysteresis loop measurements. It was observed that the value of M_s increases from 33 to 57 emu/g with increase in doping content of zinc. This behaviour is due to distribution of magnetic and non-magnetic ions of the exchange interactions such as A-B, A-A and B-B at tetrahedral and octahedral sites [20]. M_r and M_c were found to decrease with the zinc substitution with x=0.1. But for x=0.5, both M_r and M_c were found to increase. This is because, Zn^{2+} ions showed a strong preference for the tetrahedral A-site while Ni^{2+} ions showed strong preference to B-site [21].

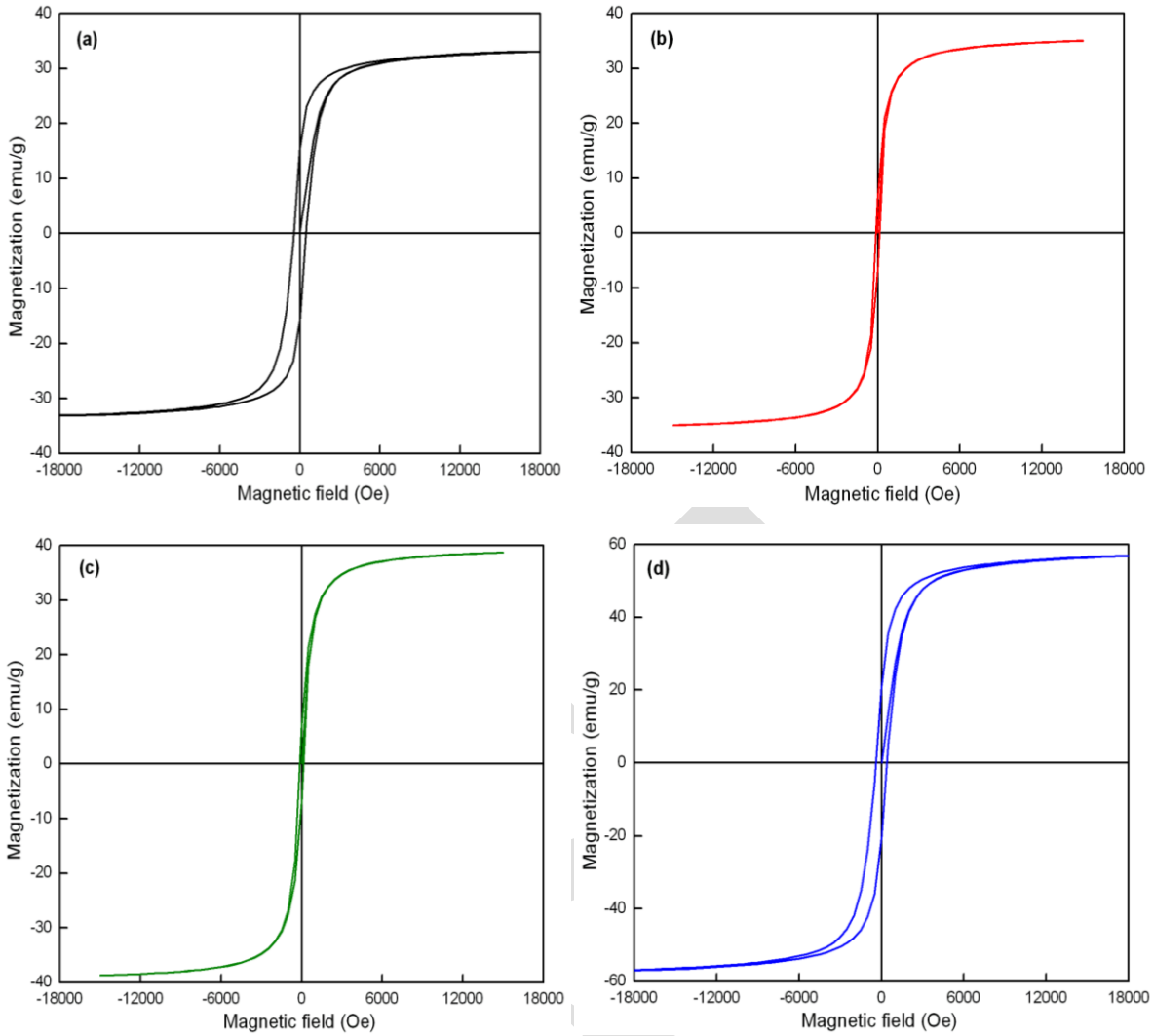

Fig.4 Magnetization versus magnetic field behaviour of (a) $NiFe_2O_4$ (b) $Ni_{0.9}Zn_{0.1}Fe_2O_4$ (c) $Ni_{0.7}Zn_{0.3}Fe_2O_4$ (d) $Ni_{0.5}Zn_{0.5}Fe_2O_4$ powders annealed at 800°C

CONCLUSION

Based on the results the following conclusions have been drawn. The nanocrystalline powders of Ni-Zn ferrite having the chemical formula $Ni_{1-x}Zn_xFe_2O_4$ ($0 \leq x \leq 0.5$) have been successfully synthesized by using sol-gel auto-combustion method, followed by heat treatment at 800°C. XRD results confirmed that all the samples have single phase spinel cubic structure. From the XRD data it is also found that crystallite size decreases with increase of zinc content. SEM image confirmed the nanocrystalline size of the host materials. The observation of FTIR absorption peaks in the range 400 cm^{-1} to 2600 cm^{-1} confirmed the occurrence of pure spinel structure. It is clear from the VSM analysis that the saturation magnetization increases with the addition non-magnetic zinc content. Based on the overall conclusion, it is recommended that it can be used as memory storage devices such as CD, TV sets, and Lap top devices.

REFERENCES

[1] P. P. Hankare, R. P. Patil, K. M. Garaadker, R. Sasikala, B. K. Chougale, Mater. Res. Bull. 46 (2011) 447.
[2] J. Giri. T. Sriharsha, D. Bhadur, J. Mater. Chem 14 (2004) 875.
[3] M. George, A. M. John, S. S. Nair, P. A. Joy, M. R. Anantharaman, J. Magn. Magn. Mater. 302 (2006) 190.
[4] H. Sato, T. Umeda, Mater. Trans. 34 (1993) 76.
[5] R. H. Arendt, J. Solid State Chem. 8 (1973) 339.
[6] S. Giri, S. Samanta, S. Maji, S. Gangli, A. Bhaumik, J. Magn. Magn. Mater. 288 (2005) 296.
[7] S. Thompson, N. J. Shircliffe, E. O. Keefe, S. Appleton, C. C. Perry, J. Magn. Magn. Mater. 292 (2005) 100.
[8] J. Wang, Mater. Sci. Eng. B. 127 (2006) 81.
[9] A. S. Albuquerque, J. D. Ardisson, W. A. A. Macedo, J. L. Lopez, R. Paniago, A. I. L. Persiano, J. Magn. Magn. Mater. 226 (2001) 1379.
[10] S. Z. Zhang, G. L. Messing, J. Am. Ceram. Soc. 73 (1990) 61.
[11] H. Shokrollahi, J. Magn. Magn. Mater. 320 (2008) 463.
[12] Muhammad Azhar Khan, Misbah ul Islam. M. Asif Iqbal, Mukhtar Ahmad, Muhammad F. Din, G. Murtaza, Ishtiaq Ahmad, Muhammad Farooq Wasi, Ceramic Inter. 884 (2014) 1356 .
[13] Ali Ghasemi, Mohammad Mousavinia, Ceramic Inter. 40 (2014) 2825.
[14] A. T. Raghavendar, Damir Pajic, Kreso Zadro, Tomislav Milekovic, P. Venkateshwar Rao, K. M. Jadhav, D. Ravinder, J. Magn. Magn. Mater. 316 (2007) 1.
[15] Khalid Mujasam Batoo, M. S. Abd El-sadek, J. of Alloys Comp. 566 (2013) 112.
[16] Navneet Singh, Ashish Agarwal, Sujata Sanghi, Paramjeet Singh, 323 (2011) 486.
[17] Mohammmed Javad Nasr Isfahani, Marjaneh Jafari Fesharaki, Vladimir Sepelak, Ceramic Inter. 39 (2013) 1163.
[18] M. Atrif, M. Nadeem, R. Grossinger, R. Satofur tell, J. of Alloys Comp. 509 (2011) 5720.
[19] P. Priyadharshini, A. Pradeep, P.Sambasiva Rao, G. Chandrasekaran, Mater. Chem. Phys. 116 (2009) 207.
[20] R. G. Gupta, R. G. Mendiratta, J Appl. Phys. 48 (1977) 2998.
[21] M. Kaiser, J. of Alloys Comp. 468 (2009) 15.